Cascading processes in the nonlinear diffraction of light by standing acoustic waves

Yu. S. Dadoenkova[*] and N. N. Dadoenkova[†]
Ulyanovsk State University, 432017 Ulyanovsk, Russian Federation

F. F. L. Bentivegna[‡]
Lab-STICC (UMR CNRS 6285), ENIB, 29238 Brest Cedex 3, France

I. L. Lyubchanskii[§]
Donetsk Physical & Technical Institute of the National Academy of Sciences of Ukraine, 83114 Donetsk, Ukraine

Y. P. Lee
Quantum Photonic Science Research Center (q-Psi) and Hanyang University, 04763 Seoul, South Korea
(Received 8 June 2015; published 12 January 2016)

The contribution of two types of cascading process to the nonlinear optical diffraction of electromagnetic waves from a standing acoustic wave in a GaAs crystal is theoretically studied. The first type of cascading process results from second-harmonic generation followed by linear acousto-optical diffraction, while the second type involves linear acousto-optical diffraction from the standing acoustic wave and subsequent sum-frequency generation. In contrast to the third, direct, nonlinear acousto-optical diffraction process we previously investigated, the photoelastic interaction between electromagnetic and acoustic waves is here linear. We establish the rules governing the cascading processes and show that in most cases the output signal simultaneously results from two or even three of the possible nonlinear diffraction mechanisms. However, we demonstrate that a careful choice of the incidence angles of the incoming electromagnetic waves, of the polarization combinations of the incoming and diffracted waves, and of the type of acoustic wave (longitudinal or transverse) makes it always possible to distinguish between the direct and either of the two cascading processes.

DOI: 10.1103/PhysRevA.93.013815

I. INTRODUCTION

Nonlinear optical methods are very useful for the investigation of the static and dynamical properties of condensed matter, not only in bulk media, but also in thin films and structured materials. In particular, if a material exhibits a periodic inhomogeneity of its properties, second-order nonlinear diffraction of electromagnetic waves (EMWs) by the resulting permittivity grating can be observed. This was investigated for the first time, both theoretically and experimentally, by Freund [1] in ferroelectrics with a laminar domain structure. Since then, similar theoretical and experimental investigations have been devoted to various periodically modulated systems, including materials with spatially modulated linear and nonlinear polarizations [2], nonlinear photonic crystals [3–9], magnetic films with regular magnetic domain structures [10–12], periodically distributed grooves [13], and nonlinear gratings [14,15].

In contrast to the aforementioned studies, it should be noted that in bulk materials it is possible to excite transient, dynamic spatially distributed inhomogeneities, e.g., through standing acoustic waves (AWs) that can induce a modulation of the second-order nonlinear optical susceptibility of a material via the nonlinear photoelastic interaction [16,17]. As a result of this modulation, a nonlinear polarization at frequency $(2\omega \pm \Omega)$ appears, where ω and Ω are the angular frequencies of the incident light and of the AW, respectively. This effect, named acoustically induced optical second-harmonic generation (SHG), was theoretically predicted in [18] and observed for the first time in GaAs [19], and later in $LiNbO_3$ [20], $CsLiB_6O_{10}$ nanocrystallites incorporated into olygoether photopolymer matrices [21], $Pb_{4.7}Ba_{0.3}Ge_3O_{11}$ [22], hydrogenated amorphous silicon films (a-Si:H) [23], InAs [24], and organometallic nanocomposites [25]. Recently, we published a theoretical investigation of nonlinear acousto-optical diffraction (NAOD), i.e., nonlinear optical diffraction from a standing AW in a bulk material in the framework of a phenomenological approach [26]. In that paper, we studied the direct interaction between two incident EMWs and a standing AW via a nonlinear photoelastic interaction [16–18]. There are, however, other ways to obtain nonlinearly diffracted EMWs from standing AWs, and the analysis of their contribution to NAOD requires the careful investigation of a two-stage cascading process, for instance the succession of the linear acousto-optic diffraction of an incident EMW from a standing AW—leading to the generation of a diffracted wave at frequency $(\omega \pm \Omega)$—and the subsequent interaction of that diffracted wave with the incident EMW. As a result, nonlinear diffraction at the same frequency $(2\omega \pm \Omega)$ as through direct NAOD [26] can be achieved. This situation was discussed in [20] from a quantum mechanical perspective as a second-order perturbative contribution to acoustically induced optical SHG.

[*]Also at Donetsk Physical & Technical Institute of the National Academy of Sciences of Ukraine, 83114 Donetsk, Ukraine, and Institute of Electronic and Information Systems, Novgorod State University, 173003 Veliky Novgorod, Russian Federation; yulidad@gmail.com

[†]Also at Donetsk Physical & Technical Institute of the National Academy of Sciences of Ukraine, 83114 Donetsk, Ukraine.

[‡]fb@enib.fr

[§]igorl@fti.dn.ua

The investigation of cascading effects in nonlinear optics has a long history starting at least from the seminal paper by Yablonovich *et al.* [27]. Since then, numerous works have been devoted to the subject (see, e.g., references in Ref. [28], which is devoted to degenerate four-wave mixing in noncentrosymmetric materials, or the chapter in [29] about multistep parametric processes in nonlinear optics). However, cascading effects in the case of NAOD have apparently not been investigated.

The goal of this paper is to present a precise theoretical analysis of NAOD from standing AWs and to compare the contributions of direct and cascading processes to the outgoing radiation. This investigation is directed at understanding how it would be possible to separate the contributions of the two mechanisms (direct and cascading) and to predict the optimal conditions for corresponding experiments, i.e., to design polarimetric and angular measurement configurations in order to distinguish between direct and cascading contributions to NAOD-generated radiation.

We illustrate our study with the numerical analysis of NAOD in a bulk GaAs crystal, because this cubic material is noncentrosymmetric, which means that optical SHG is allowed in the dipole approximation [30,31]. In practice, significant SHG yield can be obtained from a GaAs crystal in the visible and near-infrared domains. A great many papers have been devoted to the modeling and observation of SHG in uniform and patterned GaAs samples [32–35]. So far, however, no detailed account of cascading effects coupled to a standing AW appears to have been published and we believe that our study brings insight to the angular and polarimetric dependences of these mechanisms.

The paper is organized as follows. In Sec. II we briefly describe acousto-optic diffraction by standing AWs. Section III is devoted to a general description of the cascading processes and Sec. IV presents the results and the detailed discussion of our numerical calculations in the case of a GaAs crystal. The principal results are summarized in Sec. V.

II. ACOUSTO-OPTICAL DIFFRACTION BY STANDING ACOUSTIC WAVES

The study of linear light diffraction by AWs is well established, both theoretically and experimentally [36–38]. As mentioned earlier, second-order nonlinear diffraction can result from a direct process [26] or from a two-step cascade process. In each case, EMWs and an AW are coupled, and the treatment of the resulting interaction between light and sound is similar to the second-order perturbation theory of the quantum mechanical description of nonlinear acousto-optical processes [20].

A standing AW results from the interference between two traveling AWs propagating in opposite directions. If those directions are collinear to the z axis of a Cartesian system of coordinates, the displacement vector $\mathbf{u}$ in a slab of crystalline medium in which a bulk standing AW is established can be written as [39]

$$\mathbf{u}(\mathbf{r},t) = \mathbf{A}_L \cos\left(\frac{\Omega_L\, z}{v_L}\right) e^{i\Omega_L t} + \mathbf{A}_T \cos\left(\frac{\Omega_T\, z}{v_T}\right) e^{i\Omega_T t}, \quad (1)$$

where $\mathbf{A}_L = [0,0,A_z]$ and $\mathbf{A}_T = [A_x, A_y, 0]$ are the maximum magnitudes of the displacements due to the longitudinal and transverse standing AWs, respectively. The angular frequencies of these waves are denoted $\Omega_{L,T} = \pi\, v_{L,T}/L_z$, where L_z is the slab length along the z axis and $v_{L,T}$ are the wave velocities. The magnitudes of the displacement vectors vary with position z and time t, but their extrema are stationary. For each type of AW, the positions of the nodes (antinodes), i.e. the points in the crystal slab where the vibration magnitude is zero (maximal), are given by the conditions $(\Omega_{L,T}\, z)/v_{L,T} = (m + 1/2)\pi$ and $(\Omega_{L,T}\, z)/v_{L,T} = m\pi$, $m \in \mathbb{N}$, respectively. The amplitude of the displacement induced by the AW is expressed as

$$A_{L,T}^2 = \frac{2I_{\mathrm{AW}}}{\Omega_{L,T}^2\, \rho\, v_{L,T}}, \quad (2)$$

where I_{AW} is the acoustic intensity and ρ is the volumetric mass density of the material.

In the presence of SHG, fields $\mathbf{E}_\omega$ and $\mathbf{E}_{2\omega}$ of EMWs at the fundamental and second-harmonic frequencies must be taken into account and are solutions of wave equations which, in SI units, read [26]

$$\boldsymbol{\nabla} \times \boldsymbol{\nabla} \times \mathbf{E}_\omega(\mathbf{r},t) + \frac{n_\omega^2}{c}\frac{\partial^2 \mathbf{E}_\omega(\mathbf{r},t)}{\partial t^2} = -\mu_0 \frac{\partial^2 \mathbf{P}_\omega(\mathbf{r},t)}{\partial t^2}, \quad (3)$$

$$\boldsymbol{\nabla} \times \boldsymbol{\nabla} \times \mathbf{E}_{2\omega}(\mathbf{r},t) + \frac{n_{2\omega}^2}{c}\frac{\partial^2 \mathbf{E}_{2\omega}(\mathbf{r},t)}{\partial t^2} = -\mu_0 \frac{\partial^2 \mathbf{P}_{2\omega}^{\mathrm{NL}}(\mathbf{r},t)}{\partial t^2}, \quad (4)$$

where n_ω and $n_{2\omega}$ are the refractive indices of the medium at the fundamental and the second-harmonic frequencies, respectively, $\mathbf{P}_\omega(\mathbf{r},t)$ and $\mathbf{P}_{2\omega}^{\mathrm{NL}}(\mathbf{r},t)$ are the linear and second-order nonlinear polarization vectors in the crystal, c is the light velocity in vacuum, and μ_0 is the vacuum permeability. Taking the Fourier transform of Eq. (3) with respect to time and using the slowly varying envelope approximation, where $\mathbf{k}_{2\omega} \cdot \nabla \mathbf{E}(2\omega,\mathbf{r}) \gg \Delta \mathbf{E}(2\omega,\mathbf{r})$, we obtain the following reduced form [26] for the nonlinear wave equation:

$$\mathbf{k}_{2\omega} \cdot \boldsymbol{\nabla} \mathbf{E}(2\omega,\mathbf{r}) = -2i\frac{\omega^2}{c^2}\mathbf{P}^{\mathrm{NL}}(2\omega,\mathbf{r})\ \exp(i\,\mathbf{q}_{2\omega} \cdot \mathbf{r}), \quad (5)$$

where $\mathbf{E}(2\omega,\mathbf{r})$ and $\mathbf{P}^{\mathrm{NL}}(2\omega,\mathbf{r})$ are the temporal Fourier transforms of the electric field at the second-harmonic frequency and the corresponding nonlinear polarization, and

$$\mathbf{q}_{2\omega} = 2\,\mathbf{k}_\omega - \mathbf{k}_{2\omega} \quad (6)$$

is the phase-mismatch vector, $\mathbf{k}_\omega$ and $\mathbf{k}_{2\omega}$ being the wave vectors of the fundamental and second-harmonic EMWs, respectively.

In the rest of the paper, conventional summation over repeated indices $(i,j,k,l) \in \{x,y,z\}$ is assumed. In the dipole approximation the quadratic nonlinear polarization vector $\mathbf{P}^{\mathrm{NL}}(2\omega)$ in an anisotropic medium can be written in a Cartesian referential as $P_i^{\mathrm{NL}} = \chi_{ijk}^{(2)} E_j E_k$, where $\chi_{ijk}^{(2)}$ is the quadratic nonlinear optical susceptibility (NOS) tensor of the medium [20]. When a spatial modulation of the optical properties of the medium takes place, second-order contributions of elasto-optic effects to the NOS can locally be taken into account, such that

$$\chi_{ijk}^{(2)} = \chi_{ijk}^{(2,0)} + \left(\frac{\partial \chi_{ijk}^{(2)}}{\partial u_{lm}}\right)_{u_{lm}=0} u_{lm} + \cdots = \chi_{ijk}^{(2,0)} + p_{ijklm}\, u_{lm} + \cdots, \quad (7)$$

where $\chi_{ijk}^{(2,0)}$ is the NOS tensor in the absence of modulation, p_{ijklm} is the nonlinear photoelastic tensor responsible for NAOD, and u_{lm} is the strain tensor. In the linear approximation, the latter is symmetric, i.e., $u_{lm} = u_{ml}$, and its components are deduced from the local variations of the displacement vector [Eq. (1)] with

$$u_{kl}(\mathbf{r}) = \frac{1}{2}\left(\frac{\partial u_k}{\partial r_l} + \frac{\partial u_l}{\partial r_k}\right), \quad (r_k, r_l) \in \{x, y, z\}. \tag{8}$$

III. CASCADE PROCESSES

Besides the direct generation of second-harmonic radiation scattered from a standing AW previously described [26], we propose here two types of cascade processes (CPs) leading to the same result, which can phenomenologically be described as follows. In the first-type process (CP1) [Fig. 1(a)], an incoming EMW at fundamental angular frequency ω first diffracts on a standing AW (at angular frequency Ω); then the diffracted beam (angular frequency $\omega \pm \Omega$) interacts with another incoming EMW at angular frequency ω, and a sum-frequency nonlinear process produces EMWs at frequencies $2\omega \pm \Omega$. In the second-type process (CP2) [Fig. 1(b)], first SHG takes place, producing an EMW at angular frequency 2ω; then the second-harmonic wave diffracts on the standing AW, which yields EMWs at angular frequencies $2\omega \pm \Omega$. In the following, we will establish the relations necessary to the evaluation of the efficiencies of these two competing ways to produce an output signal of the angular frequencies $2\omega \pm \Omega$.

In the frequency domain, the polarization vectors involved in the first-type CP can be written as follows:

$$P_i^{(\mathrm{I})}(\omega \pm \Omega) = p_{ijkl}\, u_{kl}(\Omega)\, E_j(\omega), \tag{9}$$

$$P_i^{(\mathrm{II})}(2\omega \pm \Omega) = \chi_{ijk}^{(2)}(2\omega \pm \Omega)\, E_j(\omega)\, E_k(\omega \pm \Omega), \tag{10}$$

where superscripts (I) and (II) refer to the two consecutive subprocesses that constitute this process, namely, linear diffraction from the standing AW (stage I) and sum-frequency generation (stage II). Here p_{ijkl} and $\chi_{ijk}^{(2)}$ are elements of the linear photoelastic tensor and of the second-order NOS tensor of the crystal, respectively, and u_{kl} are elements of the strain tensor derived from the components of the displacement vector $\mathbf{u}$ [see Eq. (8)]. It is worth noting that the photoelastic interaction involved in the CPs is thus *linear*, whereas it is *nonlinear* in the case of the direct process.

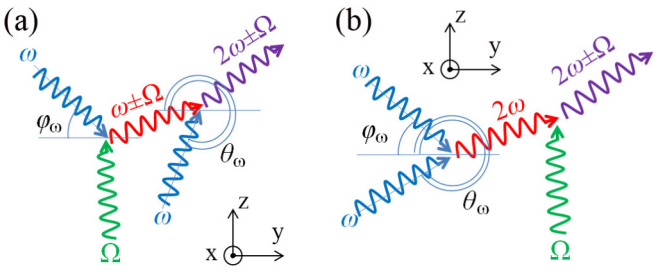

FIG. 1. Schematic of the cascade processes: (a) first-type CP (CP1): linear acousto-optical diffraction by standing AWs and sum-frequency generation; (b) second-type CP (CP2): second-harmonic generation and linear acousto-optical diffraction by standing AWs.

Analogously, for the second-type CP, the polarization vectors related to SHG (subprocess I) and diffraction from the standing AW (subprocess II) are

$$\tilde{P}_i^{(\mathrm{I})}(2\omega) = \chi_{ijk}^{(2)}(2\omega)\tilde{E}_j(\omega)\tilde{E}_k(\omega), \tag{11}$$

$$\tilde{P}_i^{(\mathrm{II})}(2\omega \pm \Omega) = p_{ijkl}u_{kl}(\Omega)\tilde{E}_j(2\omega). \tag{12}$$

The electric field components $E_i(\omega \pm \Omega)$ and $\tilde{E}_i(2\omega)$ of the EMWs generated by the first subprocesses of the first- and second-type CPs, respectively, can be obtained from the corresponding polarization terms through the following equations:

$$E_i(\omega \pm \Omega) = \frac{i\omega^2}{2c^2 k_{\omega \pm \Omega}}\left(\frac{1}{V}\int_V P_i^{(\mathrm{I})}\, e^{i\,\mathbf{q}\cdot\mathbf{r}}\, dr\right), \tag{13}$$

$$\tilde{E}_i(2\omega) = \frac{i(2\omega)^2}{2c^2 k_{2\omega}}\left(\frac{1}{V}\int_V \tilde{P}_i^{(\mathrm{I})} e^{i\,\tilde{\mathbf{q}}\cdot\mathbf{r}}\, dr\right), \tag{14}$$

where $\mathbf{q} = \mathbf{k}_\omega + \zeta - \mathbf{k}_{\omega\pm\Omega}$ and $\tilde{\mathbf{q}} = 2\mathbf{k}_\omega - \mathbf{k}_{2\omega}$ are the mismatch vectors between the wave vectors of the waves taking part in the processes, $\mathbf{k}_\omega$, $\mathbf{k}_{\omega\pm\Omega}$, and $\mathbf{k}_{2\omega}$ being the wave vectors of the fundamental, diffracted, and second-harmonic waves, respectively, and $\zeta = \Omega/v_{L,T}\ \boldsymbol{e}_z$ being the wave vector of the longitudinal (transversal) AW.

For the second stages of the first and second type of CPs the electric field strengths of the generated EMWs are, again, deduced from the associated source terms, or polarization vectors:

$$E_i(2\omega \pm \Omega) = \frac{i(2\omega \pm \Omega)^2}{2c^2 k_{2\omega\pm\Omega}}\left(\frac{1}{V}\int_V P_i^{(\mathrm{II})} e^{i\,\kappa\cdot\mathbf{r}}\, dr\right), \tag{15}$$

$$\tilde{E}_i(2\omega \pm \Omega) = \frac{i(2\omega \pm \Omega)^2}{2c^2 k_{2\omega\pm\Omega}}\left(\frac{1}{V}\int_V \tilde{P}_i^{(\mathrm{II})} e^{i\,\tilde{\kappa}\cdot\mathbf{r}}\, dr\right). \tag{16}$$

The integrals in Eqs. (13)–(16) are taken over the interaction volume V of the domain in the crystal where the average intensity (or Poynting vector) of the incident EMW is nonzero.

The mismatch vectors $\mathbf{q}$ and $\tilde{\mathbf{q}}$, as well as the quasi-phase-matching conditions for the first and second stages of each CP are given by

$$\mathbf{q} = \mathbf{k}_\omega + \zeta - \mathbf{k}_{\omega\pm\Omega} \ \text{ and } \ \kappa = \mathbf{k}_\omega + \mathbf{k}_{\omega\pm\Omega} - \mathbf{k}_{2\omega\pm\Omega} \quad \text{(CP1)}, \tag{17}$$

$$\tilde{\mathbf{q}} = 2\mathbf{k}_\omega - \mathbf{k}_{2\omega} \ \text{ and } \ \tilde{\kappa} = \mathbf{k}_{2\omega} + \zeta - \mathbf{k}_{2\omega\pm\Omega} \quad \text{(CP2)}. \tag{18}$$

For comparison, the mismatch vector for the one-stage direct NAOD process [26] obeys

$$\mathbf{q}_d = 2\mathbf{k}_\omega - \mathbf{k}_{2\omega} + \zeta, \tag{19}$$

which shows that quasi-phase-matching conditions are quite different for the CP and direct NAOD processes. The main difference between the quasi-phase-matching conditions we use and the conventional ones obtained for the theoretical description of SHG in periodically modulated structures (see, e.g., [40,41]) — or those obtained for instance with a specific experimental setup that uses the total-internal-reflection phase shift as a means to reach quasi-phase-matched SHG in a GaAs film [42]—is as follows: In the latter cases, the modulation of

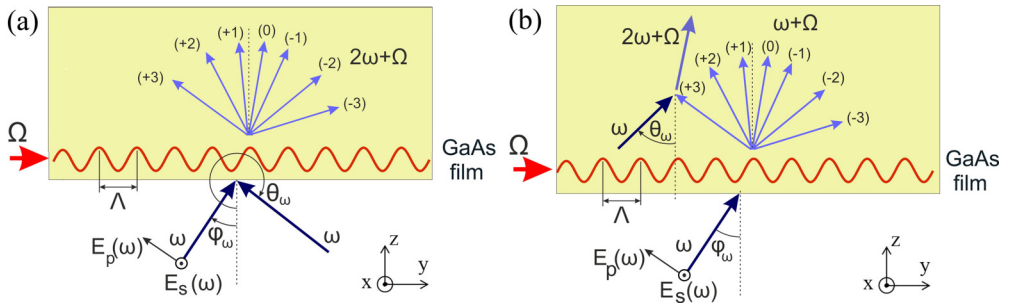

FIG. 2. Schematic of the nonlinear acousto-optical diffraction for cascading processes CP1 (a) and CP2 (b) in the transmission geometry.

the refractive indices and of the nonlinear optical susceptibility tensors is static, whereas it is time dependent in the case of NAOD. However, it can be noted that NAOD may, like the processes described in Refs. [40–42], lead to an efficient phase-matched frequency conversion process in a crystal such as GaAs thanks to the assistance of the acoustically-induced index modulation.

Moreover, the wave vectors of the EMWs diffracted by the AW must satisfy either of the Bragg conditions, i.e., $\mathbf{k}_{\omega\pm\Omega} = \mathbf{k}_{\omega} + N\mathbf{Q}_{L,T}$ or $\mathbf{k}_{2\omega\pm\Omega} = \mathbf{k}_{2\omega} + N\mathbf{Q}_{L,T}$ ($N \in \mathbb{Z}$) for CP1 and CP2, respectively, where $\mathbf{Q}_{L,T}$ are the wave vectors of the longitudinal and transverse standing AWs and N denotes the diffraction order (Fig. 2).

Phenomenologically, the field generated at frequency $2\omega \pm \Omega$ can be related to the incoming field at fundamental frequency ω through a susceptibility tensor that takes the effect of the AW into account. For CP1 and for given phase-mismatch vectors $\mathbf{q}$ and $\boldsymbol{\kappa}$ in the crystal, the s- and p-polarized components $E_{s,p}(2\omega \pm \Omega)$ of the generated field are related to those of the incoming field at the fundamental frequency as follows:

$$\begin{pmatrix} E_s(2\omega\pm\Omega,\mathbf{q},\boldsymbol{\kappa}) \\ E_p(2\omega\pm\Omega,\mathbf{q},\boldsymbol{\kappa}) \end{pmatrix} = \begin{bmatrix} \chi_{s,ss}(\mathbf{q},\boldsymbol{\kappa}) & \chi_{s,pp}(\mathbf{q},\boldsymbol{\kappa}) \\ \chi_{p,ss}(\mathbf{q},\boldsymbol{\kappa}) & \chi_{p,pp}(\mathbf{q},\boldsymbol{\kappa}) \end{bmatrix} \begin{pmatrix} E_s^2(\omega) \\ E_p^2(\omega) \end{pmatrix}. \tag{20}$$

Similarly, for CP2 and for given phase-mismatch vectors $\tilde{\mathbf{q}}$ and $\tilde{\boldsymbol{\kappa}}$ in the crystal, the s- and p-polarized components of the field $\tilde{\mathbf{E}}(2\omega \pm \Omega)$ generated at angular frequency $2\omega \pm \Omega$ depend upon those of the incoming field at the fundamental frequency:

$$\begin{pmatrix} \tilde{E}_s(2\omega\pm\Omega,\tilde{\mathbf{q}},\tilde{\boldsymbol{\kappa}}) \\ \tilde{E}_p(2\omega\pm\Omega,\tilde{\mathbf{q}},\tilde{\boldsymbol{\kappa}}) \end{pmatrix} = \begin{bmatrix} \tilde{\chi}_{s,ss}(\tilde{\mathbf{q}},\tilde{\boldsymbol{\kappa}}) & \tilde{\chi}_{s,pp}(\tilde{\mathbf{q}},\tilde{\boldsymbol{\kappa}}) \\ \tilde{\chi}_{p,ss}(\tilde{\mathbf{q}},\tilde{\boldsymbol{\kappa}}) & \tilde{\chi}_{p,pp}(\tilde{\mathbf{q}},\tilde{\boldsymbol{\kappa}}) \end{bmatrix} \begin{pmatrix} \tilde{E}_s^2(\omega) \\ \tilde{E}_p^2(\omega) \end{pmatrix}. \tag{21}$$

In Eqs. (20) and(21), the relevant components of tensors $\hat{\chi}(\mathbf{q},\boldsymbol{\kappa})$ and $\hat{\tilde{\chi}}(\tilde{\mathbf{q}},\tilde{\boldsymbol{\kappa}})$ depend on those of both the linear photoelastic tensor $\hat{p}$ and the strain tensor $\hat{u}$ of the crystal.

The numerical calculations discussed in Sec. IV are carried out for a GaAs crystal. The crystalline symmetry of that material (it belongs to the T_d point group), leaves one, two, or three nonzero elements in the (2×2) susceptibility tensors $\hat{\chi}(\mathbf{q})$ and $\hat{\tilde{\chi}}(\mathbf{q})$, depending on the polarization of the AW. Thus, for a longitudinal AW, they become

$$\begin{aligned} \hat{\chi}^{L}(\mathbf{q},\boldsymbol{\kappa}) &= \begin{bmatrix} 0 & \chi^{L}_{s,pp}(\mathbf{q},\boldsymbol{\kappa}) \\ 0 & 0 \end{bmatrix}, \\ \hat{\tilde{\chi}}^{L}(\tilde{\mathbf{q}},\tilde{\boldsymbol{\kappa}}) &= \begin{bmatrix} 0 & 0 \\ 0 & \tilde{\chi}^{L}_{p,pp}(\tilde{\mathbf{q}},\tilde{\boldsymbol{\kappa}}) \end{bmatrix}, \end{aligned} \tag{22}$$

for CP1 and CP2, respectively, whereas for a transverse AW, the corresponding tensors are

$$\begin{aligned} \hat{\chi}^{T}(\mathbf{q},\boldsymbol{\kappa}) &= \begin{bmatrix} 0 & \chi^{T}_{s,pp}(\mathbf{q},\boldsymbol{\kappa}) \\ \chi^{T}_{p,ss}(\mathbf{q},\boldsymbol{\kappa}) & \chi^{T}_{p,pp}(\mathbf{q},\boldsymbol{\kappa}) \end{bmatrix}, \\ \hat{\tilde{\chi}}^{T}(\tilde{\mathbf{q}},\tilde{\boldsymbol{\kappa}}) &= \begin{bmatrix} 0 & \tilde{\chi}^{T}_{s,pp}(\tilde{\mathbf{q}},\tilde{\boldsymbol{\kappa}}) \\ 0 & 0 \end{bmatrix}. \end{aligned} \tag{23}$$

The nonzero susceptibility tensor elements can be expressed as functions of the angles of incidence φ_ω and θ_ω of the fundamental frequency EMWs involved in any of the cascading processes (Fig. 1). It is assumed here that both incoming wave vectors belong to a plane of incidence perpendicular to the surfaces of the GaAs slab. For any given set of angles φ_ω and θ_ω, the susceptibility tensor elements appearing in Eqs. (22) and (23) assume the following form:

$$\begin{aligned} \chi^{L}_{s,pp}(\mathbf{q},\kappa) &= -\chi^{(2)}(p_{11}\sin\theta_\omega\cos\phi_\omega \\ &\quad + p_{12}\cos\theta_\omega\sin\phi_\omega)\, U_{zz}(\mathbf{q},\kappa), \qquad (24a) \\ \chi^{T}_{p,pp}(\mathbf{q},\kappa) &= 2\chi^{(2)} p_{44}\cos\phi_\omega\, U_{xz}(\mathbf{q},\kappa), \qquad (24b) \end{aligned}$$

TABLE I. Physical data for GaAs and AW parameters used for calculations.

Volumic mass	$\rho = 5.316 \times 10^{-3}\,\mathrm{kg\,cm^{-3}}$
Indices of refraction [43]	$n_\omega = 3.2919$
	$n_{2\omega} = 3.3168$
Unstrained GaAs $\hat{\chi}^{(2,0)}$ tensor element [34]	$\chi^{(2)} = 188.5 \times 10^{-12}\,\mathrm{m\,V^{-1}}$
GaAs linear photoelastic tensor elements [44]	$p_{11} = -0.165$
	$p_{12} = -0.14$
	$p_{44} = -0.072$
Acoustic wave velocities in GaAs [45]	$v_L = 4.73 \times 10^{5}\,\mathrm{cm\,s^{-1}}$
	$v_T = 3.35 \times 10^{5}\,\mathrm{cm\,s^{-1}}$
Acoustic wave intensity	$I_{\mathrm{AW}} = 30\,\mathrm{W\,cm^{-2}}$

TABLE II. Combinations of s and p polarization states of the incident and diffracted waves that can lead to $\omega \to 2\omega \pm \Omega$ nonlinear diffraction in GaAs for each diffraction mechanism and each type of AW.

	Direct NAOD [26]	CP1	CP2
Longitudinal AW	$s \to p$	$p \to s$	$p \to p$
	$p \to p$		
Transverse AW	$s \to s$	$s \to p$	$p \to s$
	$s \to p$	$p \to s$	
	$p \to s$	$p \to p$	
	$p \to p$		

$$\chi^{T}_{s,pp}(\mathbf{q},\kappa) = 2\chi^{(2)} p_{44}(\mathbf{q},\kappa)\cos(\theta_\omega - \phi_\omega) \times U_{yz}(\mathbf{q},\kappa), \tag{24c}$$

$$\chi^{T}_{p,ss}(\mathbf{q},\kappa) = 2\chi^{(2)} p_{44}\, U_{xz}(\mathbf{q},\kappa), \tag{24d}$$

$$\tilde{\chi}^{L}_{s,pp}(\tilde{\mathbf{q}},\tilde{\kappa}) = -\chi^{(2)} p_{12}(\sin\theta_\omega \cos\phi_\omega + \cos\theta_\omega \sin\phi_\omega)\, U_{zz}(\tilde{\mathbf{q}},\tilde{\kappa}), \tag{24e}$$

$$\tilde{\chi}^{T}_{s,pp}(\tilde{\mathbf{q}},\tilde{\kappa}) = -2\chi^{(2)} p_{44}(\sin\theta_\omega \cos\phi_\omega + \cos\theta_\omega \sin\phi_\omega)\, U_{xz}(\tilde{\mathbf{q}},\tilde{\kappa}). \tag{24f}$$

In Eqs. (24a)–(24f), $p_{11} = p_{xxxx} = p_{yyyy} = p_{zzzz}$, $p_{12} = p_{xxyy} = p_{xxzz} = p_{yyzz} = p_{yyxx} = p_{zzxx} = p_{zzyy}$, and $p_{44} = p_{xyxy} = p_{xzxz} = p_{yzyz} = p_{yxyx} = p_{zxzx} = p_{zyzy} = p_{xyyx} = p_{xzzx} = p_{yxxy} = p_{yzzy} = p_{zxxz} = p_{zyyz}$ denote the three nonzero components of the linear photoelastic tensor of GaAs; $\chi^{(2)} = \chi^{(2)}_{xyz} = \chi^{(2)}_{yzx} = \chi^{(2)}_{zxy} = \chi^{(2)}_{xzy} = \chi^{(2)}_{yxz} = \chi^{(2)}_{zyx}$ is the only nonzero element of the second-order susceptibility tensor of unstrained GaAs, while the functions $U_{kl}(\mathbf{q},\kappa)$ and $U_{kl}(\tilde{\mathbf{q}},\tilde{\kappa})$ derive from the strain tensor components in the spatial frequency domain obtained via Fourier transform of the real-space strain tensor components $u_{kl}(\mathbf{r})$ defined by Eq. (8). Thus,

$$u_{kl}(\gamma) = \frac{1}{V}\int_V u_{kl}(\mathbf{r}) \exp(i\,\gamma\cdot\mathbf{r})\, d\mathbf{r}, \tag{25}$$

where $\gamma \in \{\mathbf{q}, \tilde{\kappa}\}$ are the mismatch vectors involved in the relevant cascading process, and finally

$$U_{kl}(\mathbf{q},\kappa) = \frac{1}{V}u_{kl}(\mathbf{q})\int_V \exp(i\kappa\cdot\mathbf{r})d\mathbf{r}, \tag{26}$$

$$U_{kl}(\tilde{\mathbf{q}},\tilde{\kappa}) = \frac{1}{V}u_{kl}(\tilde{\kappa})\int_V \exp(i\tilde{\mathbf{q}}\cdot\mathbf{r})d\mathbf{r}, \tag{27}$$

for CP1 and CP2, respectively. The calculation procedure for the integrals which define the spectral strain tensor components $u_{kl}(\gamma)$ and functions $U_{kl}(\mathbf{q},\kappa)$ and $U_{kl}(\tilde{\mathbf{q}},\tilde{\kappa})$ in Eqs. (25)–(27) has been described in [26].

Finally, in order to estimate the relative intensities of the output diffracted waves for each CP, each type of standing AW, and each polarization configuration, one introduces the corresponding nonlinear diffraction efficiencies $D^{A}_{\alpha,\beta\beta}$ defined as

$$D^{A}_{\alpha,\beta\beta} = \frac{I(2\omega\pm\Omega)}{I^2(\omega)} \propto |\chi_{\alpha,\beta\beta}|^2, \quad (\alpha,\beta) = (s,p) \text{and} A = (L,T), \tag{28}$$

where $I(2\omega \pm \Omega)$ and $I(\omega)$ are the intensities of the output and incident beams, respectively.

IV. NUMERICAL RESULTS AND DISCUSSION

Numerical simulations discussed in this section are carried out for an incoming fundamental EMW angular frequency $\omega = 1.77 \times 10^{14}$ rad s^{-1} (i.e., for the CO_2-laser vacuum wavelength $\lambda = 10.6\,\mu$m), and for frequencies $f_{L,T} = \Omega_{L,T}/2\pi$ of the longitudinal and transverse standing AWs in the GaAs film equal to 475 and 252.5 MHz, respectively. These frequencies correspond to the same overtone value for the AW in the GaAs slab of width $L = 1\,\mu$m. The material and acoustic parameters used for calculations are presented in Table I.

Following from the form of the nonlinear susceptibility tensors [Eqs. (22) and (23)], for each cascading mechanism leading to $\omega \to 2\omega \pm \Omega$ nonlinear diffraction, and for each type of AW, only some of the potential polarization combinations ($s \to s$, $s \to p$, $p \to s$, and $p \to p$) between incident and diffracted waves are allowed by the symmetry of the crystal, as shown in Table II. Thus, three of the four combinations can be reached (and each of them through two or three of the mechanisms), $s \to s$ being the only forbidden combination for the CPs.

These results show that the type of process involved in the production of second-harmonic radiation by nonlinear diffraction cannot be deduced from the analysis of the input and output states of polarization alone. Indeed, as indicated in Table II, the $p \to p$ polarimetric combination can result from the direct NAOD process as well as from CP2 for a longitudinal AW. Similarly, for a transverse AW three combinations ($p \to p, p \to s$, and $s \to p$) can be obtained either through direct NAOD process or from CP1, and the fourth one ($p \to s$) actually takes place in all three processes. In practical terms,

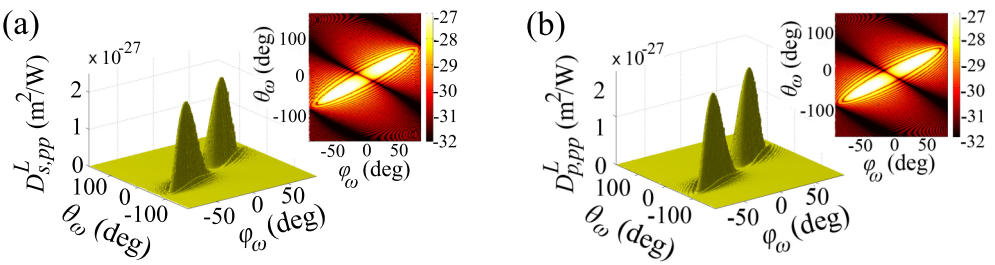

FIG. 3. Angular dependences of diffraction efficiencies $D^{L}_{s,pp}$ and $D^{L}_{p,pp}$ obtained in the zeroth order of diffraction from a longitudinal standing AW through cascading processes CP1 (a) and CP2 (b). Insets show top views of the same dependences in semilogarithmic scale.

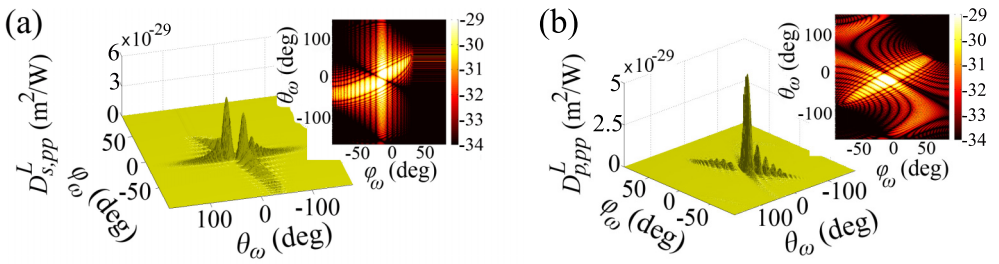

FIG. 4. Angular dependences of diffraction efficiencies $D^L_{s,pp}$ and $D^L_{p,pp}$ obtained in the first order of diffraction from a longitudinal standing AW through cascading processes CP1 (a) and CP2 (b). Insets show top views of the same dependences in semilogarithmic scale.

however, the experimental determination of the photoelastic tensor elements of the crystal requires that the mechanisms of nonlinear diffraction be unambiguously distinguished. For that purpose, in addition to selecting the type of AW and the polarization combination, one has to exploit the specific angular dependences of these mechanisms, which are presented in Figs. 3–6 for the $N = 0$ and $N = 1$ orders of diffraction.

Figure 3 thus compares diffraction efficiencies $D^L_{s,pp}$ and $D^L_{p,pp}$ obtained in the zeroth order of diffraction from a longitudinal standing AW through cascading processes CP1 [Fig. 3(a)] and CP2 [Fig. 3(b)], respectively, as functions of the angles of incidence φ_ω and θ_ω of the incident waves at the fundamental frequency (as defined in Fig. 1). Top-views of the same dependences are given as insets in semilogarithmic scale. Figure 4 shows the same parameters for the first order of diffraction. Thus the angular dependences of both $p \to s$ and $p \to p$ combinations exhibit the same double broad peaks in the zeroth order, but while the $p \to s$ combination can unambiguously be attributed to the CP1 process, the $p \to p$ combination can indeed result from either the CP2 or the direct process (see Table II).

In comparison, the angular dependences of $D^L_{s,pp}$ and $D^L_{p,pp}$ in the first order of diffraction are clearly different, as evidenced by Figs. 4(a), with two main diffraction peaks for CP1, and 4(b), with a single sharp peak for CP2. The magnitudes of diffraction efficiencies decrease (by two orders of magnitudes) between the zeroth and the first orders of diffraction. Consequently, the study of the first order of diffraction unambiguously lifts any uncertainty when it comes to attributing the diffracted signal to a specific mechanism.

For a transverse standing AW, calculations show that the angular dependences of the three $D^T_{\alpha,\beta\beta}$ $(\alpha,\beta) = (s,p)$ diffraction efficiencies associated with the three possible polarization combinations allowed by the CP1 process are almost identical. Their angular behavior, however, clearly differs from that of the CP2 process for the $p \to s$ combination, i.e., the only one that the latter process allows, as evidenced by Figs. 5 and 6 for the zeroth and first orders of diffraction, respectively, in which $D^T_{s,pp}$ obtained through either the CP1 mechanism [Figs. 5(a) and 6(a)] or the CP2 mechanism [Figs. 5(b) and 6(b)] is presented. In addition, it must be noted that the respective angular dependences of the CPs are also different from that of the direct process, which allows the $p \to s$ combination as well. Moreover, in contrast to the case of a longitudinal standing AW, the values of the diffraction peaks are of a similar order of magnitude in the zeroth and first diffraction orders.

Overall, the various processes of the nonlinear diffraction by a standing AW also differ from each other in the magnitude of their efficiencies, depending on whether they are mediated by a longitudinal or a transverse AW. A comparison of Figs. 3–6 shows that the process efficiencies for a transverse AW are three (respectively, four to five) orders of magnitude larger than those for a longitudinal AW in the zeroth (respectively, the first) order of diffraction.

As indicated in Table II, and as was demonstrated in [26], the direct process for the observation of nonlinear diffraction from a standing AW is allowed for all four polarization combinations with a transverse AW, and for two of them ($s \to p$ and $p \to p$) with a longitudinal AW. This means that in most cases the output signal at frequency $2\omega \pm \Omega$ stems from two or even three simultaneous processes. However, as mentioned above, a careful choice of the incidence angles of the incoming waves and of the polarization combinations and type of AW makes it always possible to distinguish between the three processes. As a consequence, it can be expected that experimental measurements carried out with a sufficient number of such experimental parameters, and confronted with our calculations, can lead to an estimate of the values of the

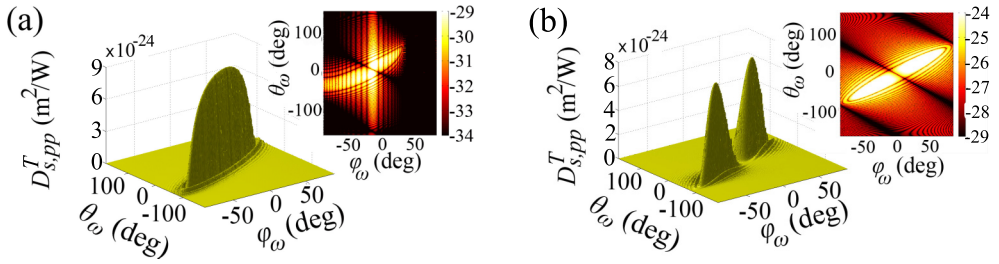

FIG. 5. Angular dependences of diffraction efficiency $D^T_{s,pp}$ obtained in the zeroth order of diffraction from a transverse standing AW through cascading processes CP1 (a) and CP2 (b). Insets show top views of the same dependences in semilogarithmic scale.

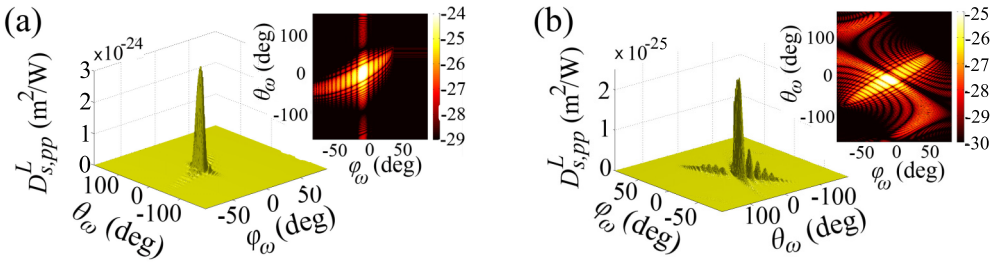

FIG. 6. Angular dependences of diffraction efficiency $D^T_{s,pp}$ obtained in the first order of diffraction from a transverse standing AW through cascading processes CP1 (a) and CP2 (b). Insets show top views of the same dependences in semilogarithmic scale.

nonlinear susceptibility tensor elements, as well as those of the linear and nonlinear photoelastic tensor elements of GaAs or any other crystal of the same symmetry group—provided that it is sufficiently transparent at both the fundamental and the second-harmonic frequencies.

V. CONCLUSIONS

In this paper, we have investigated the contribution of two types of cascading processes to the nonlinear optical diffraction of electromagnetic waves from a longitudinal or transverse standing acoustic wave established in a GaAs crystal. Contrary to the direct process described in detail in our previous publication [26], the photoelastic interaction between electromagnetic and acoustic waves is here linear. The first type thus results from the succession of linear acousto-optical diffraction and sum-frequency generation. The second type of cascading process involves a nonlinear optical process, second-harmonic generation, followed by linear acousto-optical diffraction. The phase-matching conditions for these two mechanisms are different, which accounts for the clear specificity of their respective angular dependences with respect to the angles of incidence of the interacting electromagnetic waves. Moreover, the very existence of these processes, as well as their efficiency and angular behavior, also depends on the nature (longitudinal or transverse) of the acoustic wave that mediates the linear photoelastic process, and on the states of polarization of the incoming and diffracted electromagnetic waves. We have carefully established in great detail all the rules governing the dependence of the cascading processes upon such parameters, and compared them to those previously obtained for the direct mechanism. As a result, our simulations can be confronted with a set of well-chosen measurements (in terms of incidence angles of the incoming waves, input and output polarization combinations, and type of acoustic wave) in order to determine the values of the nonlinear susceptibility tensor elements, as well as those of the linear photoelastic tensor elements of any crystal belonging to the same symmetry group as GaAs. Furthermore, carrying out similar calculations for crystals with a different type of symmetry does not present any particular difficulties.

ACKNOWLEDGMENTS

This research is supported partly by the European Union's Horizon 2020 research and innovation program under the Marie Skłodowska-Curie Grant Agreement No. 64434 "MagIC" (Yu.S.D., N.N.D., and I.L.L.) and the MPNS COST Action MP1403 "Nanoscale Quantum Optics" (Yu.S.D., N.N.D., and I.L.L.), and also is supported by a grant (Project No. 14.Z50.31.0015) from the Ministry of Education and Science of the Russian Federation (Yu.S.D., N.N.D.). Three of the authors (Yu.S.D., N.N.D., and I.L.L.) are very grateful to École Nationale d'Ingénieurs de Brest (France) for its financial support (Grant No. 14MOESMOMO14).

[1] I. Freund, Phys. Rev. Lett. **21**, 1404 (1968).
[2] V. A. Belyakov, JETP Lett. **70**, 811 (1999).
[3] V. Berger, Phys. Rev. Lett. **81**, 4136 (1998).
[4] A. M. Malvezzi, F. Cattaneo, G. Vecchi, M. Falasconi, G. Guizzetti, L. C. Andreani, F. Romanato, L. Businaro, E. Di Fabrizio, A. Passaseo, and M. De Vittorio, J. Opt. Soc. Am. B **19**, 2122 (2002).
[5] A. A. Fedyanin, O. A. Aktsipetrov, D. A. Kurdyukov, V. G. Golubev, and M. Inoue, Appl. Phys. Lett. **87**, 151111 (2005).
[6] A. Arie and N. Voloch, Laser Photon. Rev. **4**, 355 (2010).
[7] W. Wang, Y. Sheng, V. Roppo, Z. Chen, X. Niu, and W. Krolikowski, Opt. Express **21**, 18671 (2013).
[8] A. Arie, A. Bahabad, and N. Habshoosh, in *Ferroelectric Crystals for Photonic Applications*, edited by P. Ferraro, S. Grilli, and P. De Natale, Springer Series in Material Science Vol. 91 (Springer, Berlin, 2009), Chap. 10, pp. 259–284.
[9] K. Kalinowski, A. Shapira, A. Libster-Hershko, and A. Arie, Opt. Lett. **40**, 13 (2015).
[10] N. N. Dadoenkova, I. L. Lyubchanskii, M. I. Lyubchanskii, and Th. Rasing, Appl. Phys. Lett. **74**, 1880 (1999).
[11] I. L. Lyubchanskii, N. N. Dadoenkova, M. I. Lyubchanskii, E. A. Shapovalov, A. E. Zabolotin, K. Y. Guslienko, and Th. Rasing, Appl. Phys. B: Lasers Opt. **74**, 711 (2002).
[12] N. N. Dadoenkova, I. L. Lyubchanskii, M. I. Lyubchanskii, E. A. Shapovalov, A. E. Zabolotin, and Th. Rasing, J. Opt. Soc. Am. B **22**, 215 (2005).
[13] S. V. Lazarenko, A. Kirilyuk, Th. Rasing, and J. C. Lodder, J. Appl. Phys. **93**, 7903 (2003).
[14] S. M. Saltiel, D. N. Neshev, W. Krolikowski, A. Arie, O. Bang, and Yu. S. Kivshar, Opt. Lett. **34**, 848 (2009).
[15] S. M. Saltiel, D. N. Neshev, W. Krolikowski, N. Voloch-Bloch, A. Arie, O. Bang, and Yu. S. Kivshar, Phys. Rev. Lett. **104**, 083902 (2010).

[16] M. Lax and D. F. Nelson, Phys. Rev. B **4**, 3694 (1971).
[17] D. F. Nelson and M. Lax, Phys. Rev. B **3**, 2795 (1971).
[18] J.-W. Jeong, S.-C. Shin, I. L. Lyubchanskii, and V. N. Varyukhin, Phys. Rev. B **62**, 13455 (2000).
[19] G. D. Boyd, F. R. Nash, and D. F. Nelson, Phys. Rev. Lett. **24**, 1298 (1970).
[20] P. N. Keating and Ch. Deutsch, Phys. Rev. B **3**, 3531 (1971).
[21] A. Majchrowski, I. V. Kityk, T. Łukasiewicz, A. Mefleh, and S. Benet, Opt. Mater. **15**, 51 (2000).
[22] I. V. Kityk, J. Zmija, A. Majchrowski, and J. Ebothe, J. Appl. Phys. **93**, 1160 (2003).
[23] J. Ebothe, I. V. Kityk, P. Roca i Cabarrocas, C. Godet, and B. Equer, J. Phys. D: Appl. Phys. **36**, 713 (2003).
[24] M. Makowska-Janusik, K. J. Plucinski, A. Hruban, J. Ebothe, I. Fuks-Janczarek, and I. V. Kityk, Semicond. Sci. Technol. **19**, 1285 (2004).
[25] A. Migalska-Zalas, B. Sahraoui, I. V. Kityk, S. Tkaczyk, V. Yuvshenko, J.-L. Fillaut, J. Perruchon, and T. J. J. Muller, Phys. Rev. B **71**, 035119 (2005).
[26] N. A. Shevchenko, N. N. Dadoenkova, I. L. Lyubchanskii, F. F. L. Bentivegna, Y. P. Lee, and Th. Rasing, Photonics Nanostruct. Fundam. Appl. **10**, 400 (2012).
[27] E. Yablonovich, C. Flytzanis, and N. Bloembergen, Phys. Rev. Lett. **29**, 865 (1972).
[28] I. Biaggio, Phys. Rev. A **64**, 063813 (2001).
[29] S. M. Saltiel, A. A. Sukhorukov, and Yu. S. Kivshar, in *Progress in Optics*, Vol. 47, edited by E. Wolf (Elsevier, Amsterdam, 2005).
[30] Y. R. Shen, *The Principles of Nonlinear Optics* (Wiley, New York, 1984).
[31] R. W. Boyd, *Nonlinear Optics* (Academic Press, San Diego, 1992).
[32] S. Bergfeld and W. Daum, Phys. Rev. Lett. **90**, 036801 (2003).
[33] M. B. Oron, S. Pearl, P. Blau, and S. Shusterman, Opt. Lett. **35**, 2678 (2010).
[34] D. de Ceglia, G. D'Aguanno, N. Mattiucci, M. A. Vincenti, and M. Scalora, Opt. Lett. **36**, 704 (2011).
[35] L. P. Gonzalez, D. C. Upchurch, P. G. Schunemann, L. Mohnkern, and S. Guha, Opt. Lett. **38**, 320 (2013).
[36] M. Born and E. Wolf, *Principles of Optics* (Cambridge University Press, Cambridge, 1999), 7th ed.
[37] Yu. V. Gulyaev, V. V. Proklov, and G. N. Shkerdin, Sov. Phys. Usp. **21**, 29 (1978).
[38] A. Korpel, *Acousto-Optics* (Marcel Dekker, New York, 1997), 2nd ed.
[39] L. D. Landau and E. M. Lifshitz, *Theory of Elasticity* (Pergamon Press, Oxford, 1970), 2nd ed.
[40] M. M. Fejer, G. A. Magel, D. H. Jundt, and R. L. Byer, IEEE J. Quantum Electron. **28**, 2631 (1992).
[41] A. Fiore, V. Berger, E. Rosencher, P. Bravetti, and J. Nagle, Nature (London) **391**, 463 (1998).
[42] H. Komine, W. H. Long, Jr., J. W. Tully, and E. A. Stappaerts, Opt. Lett. **23**, 661 (1998).
[43] A. H. Kachare, W. G. Spitzer, and J. E. Fredrickson, J. Appl. Phys. **47**, 4209 (1976).
[44] *Handbook of Optical Materials*, edited by M. J. Weber (CRC Press, New York, 2003).
[45] S. Adachi, J. Appl. Phys. **58**, R1 (1985).